Temperature-induced abrupt volume inflation in the mixed-valence ternary Zintl phase $Yb_8Ge_3Sb_5$†

Serena Margadonna,*[a] Kosmas Prassides,*[b] Maria Chondroudi,[c] James R. Salvador[c] and Mercouri G. Kanatzidis*[c]

Received (in Cambridge, UK) 15th August 2005, Accepted 29th September 2005
First published as an Advance Article on the web 20th October 2005
DOI: 10.1039/b511606f

The Zintl phase, $Yb_8Ge_3Sb_5$ exhibits a complex lattice response and an abrupt negative thermal expansion below 15 K – subtle structural changes before and after the transition are consistent with temperature-induced electron transfer from (to) Yb 4*f* bands to (from) Sb 5*p* and Ge 4*p* bands.

Zintl phases have provided a fertile research field for many decades, yielding systems of remarkable diversity in both structural and electronic properties.[1] They comprise combinations of electropositive metallic elements (*e.g.* alkali, alkaline earth) and more electronegative metalloids (*e.g.* elements of groups 13 to 15). Recent synthetic efforts have been directed towards including rare-earth elements in the *A* cation sublattice of Zintl phases.[2] Of particular importance are those elements which support mixed valence, such as Ce, Sm, Eu, Tm, and Yb. Such rare-earth Zintl phases could potentially provide a link with one of the most fascinating classes of strongly correlated systems – intermediate valence Kondo insulators and heavy fermions – which currently attract broad experimental and theoretical interest. Intermediate-valence in rare earth systems[3] arises when 4*f* electron correlations become dominant and the $4f^n$ and $4f^{n-1}5d^1$ configurations are nearly degenerate and lie close to the Fermi energy. Alternatively, the simultaneous presence of an electronically active anion sublattice can act as an electron reservoir which can accept electrons from or donate electrons to the rare earth 4*f* bands with changes in temperature or pressure, thereby modulating the valence of the rare earth sublattice. Rare earth compounds which show temperature- or pressure-induced valence changes include binary chalcogenides (SmS, SmSe),[4] ternary intermetallics ($YbInCu_4$, YbGaGe),[5,6] and fulleride salts ($Sm_{2.75}C_{60}$, $Yb_{2.75}C_{60}$).[7]

$Yb_8Ge_3Sb_5$ is an intriguing mixed-valent Zintl phase[8] that features only homoatomic bonds among its constituent Ge and Sb metalloids (Fig. 1). According to the Zintl–Klemm concept of formal charge assignment, mixed valence is encountered for all three components into which the structure can be decomposed. The Ge sublattice comprises a quasi-1D infinite chain of edge-sharing tetrahedra [$(4b\text{-}Ge^0)(2b\text{-}Ge^{2-})_2$]. The Sb sublattice consists of lines of $(Sb^{2-})_2$ dimeric species and isolated Sb^{3-} anions, while the remaining species are Yb^{2+} and mixed valence $Yb^{2+/3+}$ cations.

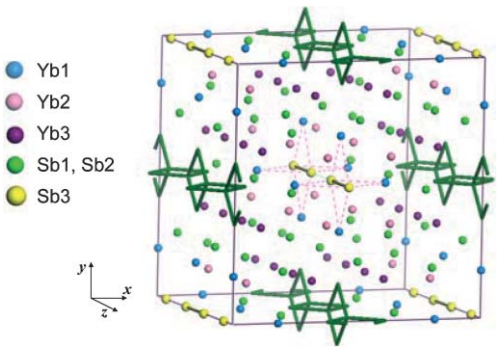

Fig. 1 Tetragonal crystal structure of $Yb_8Ge_3Sb_5$. The infinite chains of edge-sharing Ge_3 tetrahedra and $Sb(3)_2$ dimers are depicted in dark green and yellow, respectively. The isolated Yb(1), Yb(2), Yb(3), Sb(1) and Sb(2) ions are also labelled.

A reasonable formal charge-balanced formula was written as $(Yb^{2+})_6(Yb^{3+})_2(Ge_3)^{4-}(Sb^{3-})_4(Sb^{2-})$.[8] Here we report an unexpected negative volume expansion occurring abruptly in $Yb_8Ge_3Sb_5$ when it is cooled to 15 K. Synchrotron X-ray powder diffraction studies show that the structural response to change in temperature is a complex process and implies a strong coupling between the electronic (valence) degrees of freedom of the anion and cation sublattices.

Inspection of the synchrotron X-ray diffraction profiles of powder $Yb_8Ge_3Sb_5$ samples‡ at 300 K confirmed the body-centred tetragonal unit cell (space group *I*4/*mmm*) of $Yb_8Ge_3Sb_5$. Based on the evolution of the diffraction profiles down to 15 K the refined structure remained strictly tetragonal with both lattice constants, *a* and *c* decreasing smoothly (Fig. 2). The rate of contraction at 10.9 and 19.4 ppm K^{-1} for the *a* and *c* lattice constants, respectively is considerably anisotropic and leads to a gradual increase of the (*a*/*c*) ratio with decreasing temperature. However, the lattice response to further decrease in temperature below 15 K is dramatically different. The diffraction peaks suddenly shift to lower angles on cooling (Fig. 3), implying an anomalous structural behaviour whereby the material rapidly expands as the temperature decreases to 5 K (negative thermal expansion). Remarkably, the unit cell volume achieved at 5 K is notably larger than that at 300 K. Besides the shifts in peak positions, no changes in relative peak intensities are apparent as the lattice inflates, consistent with an isosymmetric phase transition.

The widths of *all* diffraction peaks increase at the same temperature (10 K) at which the sign of the thermal expansivity becomes negative and then they somewhat decrease on further cooling to 5 K. This broadening could reflect the presence of a

[a]*School of Chemistry, University of Edinburgh, Edinburgh, UK EH9 3JJ. E-mail: serena.margadonna@ed.ac.uk*
[b]*Department of Chemistry, University of Durham, Durham, UK DH1 3LE. E-mail: K.Prassides@durham.ac.uk*
[c]*Department of Chemistry, Michigan State University, East Lansing, Michigan, 48824, USA. E-mail: kanatzidis@chemistry.msu.edu*
† Electronic supplementary information (ESI) available: results of the structural refinements. See DOI: 10.1039/b511606f

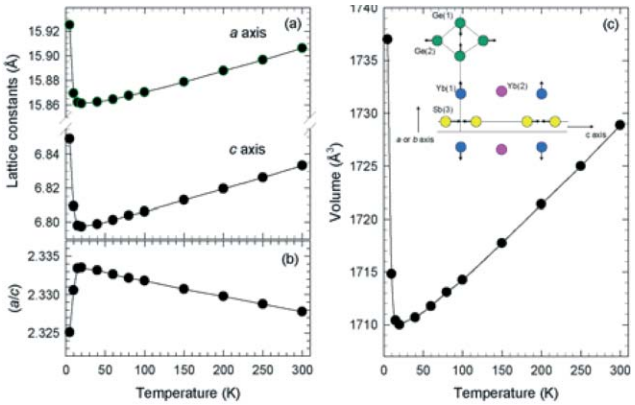

Fig. 2 Temperature evolution of (a) the tetragonal lattice constants *a* and *c*, (b) the ratio (*a*/*c*) and (c) the unit cell volume, *V* in $Yb_8Ge_3Sb_5$. The inset in (c) shows a schematic representation of the temperature response of the Yb(1), Sb(3) and Ge sublattices. The colour scheme is as in Fig. 1.

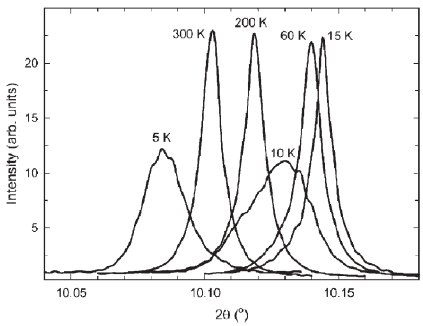

Fig. 3 Selected region of the diffraction profile of $Yb_8Ge_3Sb_5$ showing the temperature evolution of the (422) Bragg reflection (λ = 0.42976 Å). The peak shifts monotonically to higher angles (lattice contraction) on heating from 5 to 15 K and then to lower angles (lattice expansion) on further heating to room temperature.

structural transition undetectable even with the ultrahigh resolution of the present measurements. More likely it could reflect the appearance of strain effects and local structural inhomogeneities accompanying the rapid structural transformation. Rietveld refinements of the diffraction data at 10 and 5 K were thus performed successfully with the same tetragonal model employed in the higher temperature range (at 5 K: a = 15.92501(4) Å, c = 6.84918(3) Å, R_{wp} = 5.10%, R_{exp} = 2.43%, Fig. 2S, Table 1S). The temperature evolution of the lattice constants and of the unit cell volume between 5 and 300 K is shown in Fig. 2. As a result of the isosymmetric phase transition below 15 K, the overall volume increases by $\delta V/V$ = 1.55% at 5 K and the lattice dimensions at this temperature become even larger than those at ambient temperature. The expansion is again strongly anisotropic with a much smaller temperature response of the basal plane than that of the unique *c* axis ($\delta a/a$ = 0.40%, $\delta c/c$ = 0.75%).

The phenomenology in the unit cell metrics below 15 K is strongly reminiscent of the behaviour of mixed valence rare earth solids that undergo abrupt +2 ↔ +3 valence transitions with changes in temperature or pressure.[3–7] Because of the differing ionic size ($r_{+2} > r_{+3}$) of the two Yb valence states, the isosymmetric valence transitions result in drastic volume changes (large expansion or contraction accompanies reduction or oxidation, respectively).

In order to understand the origin of the anomalous NTE behaviour of $Yb_8Ge_3Sb_5$, we examine in detail the temperature evolution of the structural parameters. The cation sublattice comprises three symmetry-inequivalent Yb ions (Fig. 1), whose oxidation states at room temperature can formally be assigned as +2 (Yb(1), Yb(2)) and mixed valence, nominally +2.5 (Yb(3)), respectively. Though an $Yb^{2.5+} \rightarrow Yb^{2+}$ valence transition of the Yb(3) sublattice on cooling < 15 K would be consistent with the observed lattice response, there is little evidence of a substantial change in the Yb(3) coordination environment – the bond distances to the nearest Ge and Sb neighbours only increase by about 0.01–0.02 Å below 15 K (Fig. 3S), insufficient to account for the large increase in the overall lattice size.

We thus turn our attention to the anion sublattice components. These include isolated Sb^{3-} ions (Sb(1), Sb(2)) and Sb(3) chains running along the *c* axis of the unit cell. The latter show alternating short (3.37(1) Å) and long (3.46(1) Å) interatomic contacts at room temperature. As the distance between two isolated Sb atoms of 3.37 Å is too short to be non-bonding, the chains can be described as comprising $^1_\infty[Sb^{2-}\cdots Sb^{2-}]$ dimers in which the Sb–Sb bond order is considerably less than 1 (*cf.* Sb–Sb distance in elemental Sb is 2.9 Å). Fig. 4a shows the temperature evolution of the two Sb(3)–Sb(3) bond lengths. A striking feature of this plot is that while the interdimer distance continuously contracts on cooling between 300 and 15 K as expected, the intradimer distance shows a smooth expansion. As a result, at low temperatures (15–20 K) the two distances are essentially identical within experimental error at 3.40 Å, resulting in an apparently undistorted homoatomic $^1_\infty[\cdots Sb^{2-}\cdots]$ chain. On cooling further below 15 K, the distortion reappears and the weakly bonded $Sb^{2-}\cdots Sb^{2-}$ dimers reform, coinciding with the onset of the abrupt lattice expansion.

The second distinct anion sublattice is the infinite chain of edge-sharing tetrahedra composed of the $^1_\infty[Ge_3]^{4-}$ Zintl anions, also

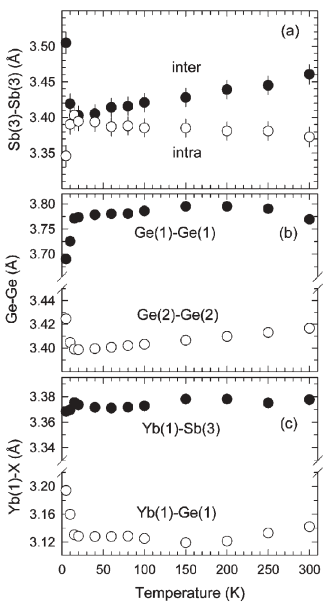

Fig. 4 Temperature dependence of selected interatomic distances in $Yb_8Ge_3Sb_5$. (a) Intra- and inter-dimer Sb(3)–Sb(3) distances for the $^1_\infty[Sb^{2-}\cdots Sb^{2-}]$ chain. (b) 2b-[Ge(1)–Ge(1)] and 4b-[Ge(2)–Ge(2)] separations for the $^1_\infty[Ge_3]^{4-}$ chain. (c) Interatomic separations between Yb(1) and the $^1_\infty[Sb^{2-}\cdots Sb^{2-}]$ and $^1_\infty[Ge_3]^{4-}$ Zintl anions.

propagating along the *c* axis. The tetrahedrally coordinated 4b-Ge(2) atoms (oxidation state 0) lie in special positions (½,0,¼) and therefore, the temperature dependence of the Ge(2)–Ge(2) distance simply mirrors that of the *c* lattice constant (Fig. 4b). On the other hand, the bridging 2b-Ge(1) atoms (oxidation state −2) respond differently to the decrease in temperature below 15 K and the Ge(1)–Ge(1) distance displays a sharp and substantial decrease at the transition temperature (from 3.77 Å to 3.69 Å). The combined effect of the expanded Ge(2)–Ge(2) and contracted Ge(1)–Ge(1) distances is a shorter Ge(1)–Ge(2) bond as reflected by a decrease of ~0.02 Å of the bond lengths.

The environment of $Yb(1)^{2+}$ and $Yb(2)^{2+}$ cations also shows a temperature dependence. Each Yb(1) cation lying along the *a* or *b* axes bridges the $^1_\infty[Sb^{2-}\cdots Sb^{2-}]$ and $^1_\infty[Ge_3]^{4-}$ Zintl anions, which run along the *c* axis, by straddling the intradimer $Sb(3)^{2-}\cdots Sb(3)^{2-}$ bonds on one side and coordinating to the 2b-Ge(1) anions at a distance of 3.14 Å directly opposite (Fig. 2 inset). The Yb(1)–Sb(3) separation shows little temperature dependence remaining throughout at ~3.37 Å, despite the considerable changes in the Sb(3)–Sb(3) bond distances (Fig. 4c). On the other hand, the Yb(1)–Ge(1) separation suddenly elongates by ~0.08 Å below 15 K, as the Ge(1)–Ge(1) distance shortens. Finally, the response of the Yb(2) near-neighbour coordination environment to temperature simply mirrors that of the unit cell dimensions, contracting smoothly down to 15 K and then suddenly inflating (Fig. 3S).

The most prominent point arising from the present structural refinements is the remarkable response of the unit cell metrics at low temperatures. The NTE and abrupt collapse (by 1.55%) of the structure of $Yb_8Ge_3Sb_5$ on heating from 5 to 15 K are not accompanied by a change in space group symmetry. The origin of these effects should be electronic and can be sought in the fragility of the valence states of Yb and its tendency to exhibit mixed valency. A critical clue for the elucidation of the anomalous overall structural response and its relationship to changes in the electronic structure comes from the data on the Sb(3)–Sb(3) fragments. We suggest that the Sb–Sb bond distance alternation along *c* at room temperature can be interpreted as arising from a classic Peierls distortion of a monoatomic $^1_\infty[\cdots Sb^{2-}\cdots]$ chain with a partially filled 5*p* electronic band. The magnitude of the distortion progressively decreases with decreasing temperature as the intradimer $[Sb^{2-}\cdots Sb^{2-}]$ separation increases. Such elongation and concomitant bond weakening can arise from the spilling over of electron density from the Yb(1) sublattice into the Sb 5*p* states – *i.e.* Yb(1) is progressively oxidised from +2 to a mixed valence state of $+(2+\varepsilon)$ on cooling from 300 to 15 K. Then in the vicinity of 15 K, the distortion is essentially suppressed and the Sb(3) homoatomic chain comprises equidistant open-shell Sb^{2-} ions. As this 1D arrangement is inherently electronically unstable, the solid abruptly responds and the Peierls distortion to a dimerised chain is re-established. At the same time, Yb(1) is reduced back to the +2 valence and its ionic size suddenly increases, leading to the observed large NTE. The transition occurring at this temperature is reminiscent of a facile, spring-like action that seems to lead to an "overshoot" in volume expansion to a value larger than that at room temperature.

As the Yb(1) sublattice also couples to the Ge sublattice (Fig. 2c inset), the lattice expansion below 15 K is also reflected in the coordination of the edge-sharing $[Ge_3]^{4-}$ tetrahedra whose size sharply contracts. This could also imply charge transfer from the Yb(1) 4*f* bands towards the Ge 4*p* bands in tandem with the corresponding process of electron transfer into the Sb(3) sublattice.

In conclusion, the ternary Zintl phase $Yb_8Ge_3Sb_5$ exhibits an unusually complex structural and electronic response to changes in temperature. To explain the observed gradual disappearance of the bond length alternation in the $^1_\infty[Sb^{2-}\cdots Sb^{2-}]$ chains on cooling from ambient temperature and the subsequent sudden redimerisation and abrupt NTE of the unit cell size below 15 K, we have invoked effects of electronic origin, associated with the tendency of Yb to exhibit mixed valence character. The results reported here imply that similar phenomena may be encountered in Yb compounds in which atomic motions within a relatively loosely packed soft lattice are possible.

We thank the ESRF for synchrotron X-ray beamtime, the Royal Society for a Dorothy Hodgkin Research Fellowship (S.M.), the Department of Energy for financial support (DE-FG02-99ER45793) and Dr Fitch (ESRF) for help with the experiments.

Notes and references

‡ $Yb_8Ge_3Sb_5$ was prepared as follows. 0.17304 g (1 mmol) of Yb, 0.0272 g (0.375 mmol) of Ge and 0.0761 g (0.625 mmol) of Sb were combined and cold pressed into a pellet which was loaded in a carbon-coated 13 mm quartz tube and subjected to the following protocol: heated to 850 °C in 10 h, held at 850 °C for 72 h, and cooled to 50 °C in 12 h. For the synchrotron X-ray diffraction measurements, samples were sealed in thin-wall capillaries (d = 0.5 mm). Diffraction data (λ = 0.42976 Å) were collected on heating between 5 and 300 K (using a continuous-flow cryostat) with the high-resolution powder diffractometer on beamline ID31 at the ESRF, Grenoble, France and were rebinned in the range 2°–25° to a 0.001° step. Data analysis was performed with the GSAS suite of Rietveld analysis programs. Peaks arising from impurity phases were excluded from the refinements. The very high resolution of the data allowed us to proceed smoothly with the Rietveld refinement of the diffraction profiles, after excluding the contributions from the impurity peaks and derive reliable lattice constants and structural parameters (at 300 K: a = 15.90621(5) Å, c = 6.83324(3) Å, agreement factors: R_{wp} = 6.76%, R_{exp} = 2.74%, Fig. 1S).

1 S. M. Kauzlarich, *Chemistry, Structure and Bonding of Zintl Phases and Ions*, VCH, New York, NY, 1996.
2 E. A. Leon-Escamilla, W. M. Hurng, E. S. Peterson and J. D. Corbett, *Inorg. Chem.*, 1997, **36**, 703; R. Lam, R. McDonald and A. Mar, *Inorg. Chem.*, 2001, **40**, 952; A. Bentien, A. Palmqvist, D. Bryan, S. Latturner, G. D. Stucky, L. Furenlid and B. Iversen, *Angew. Chem.*, 2000, **39**, 3613; A. C. Payne, M. M. Olmstead, S. M. Kauzlarich and D. J. Webb, *Chem. Mater.*, 2001, **13**, 1398; J. Y. Chan, M. M. Olmstead, S. M. Kauzlarich and D. J. Webb, *Chem. Mater.*, 1998, **10**, 3583; S.-J. Kim, J. Salvador, D. Bilc, S. D. Mahanti and M. G. Kanatzidis, *J. Am. Chem. Soc.*, 2001, **123**, 12704; J. Y. Chan, M. M. Olmstead, H. Hope and S. M. Kauzlarich, *J. Solid State Chem.*, 2000, **155**, 168; M. A. Zhuravleva, J. Salvador, D. Bilc, S. D. Mahanti, J. Ireland, C. R. Kannewurf and M. G. Kanatzidis, *Chem.-Eur. J.*, 2004, **10**, 3197.
3 P. Wachter, in K. A. Gschneidner, L. Eyring, G. H. Lander and G. R. Chopin (Eds.): *Handbook on the Physics and Chemistry of Rare Earths*, North Holland, Amsterdam, 1994, Vol. 19, p. 177.
4 A. Jayaraman, E. Bucher, P. D. Dernier and L. D. Longinotti, *Phys. Rev. Lett.*, 1973, **31**, 700; A. Jayaraman, V. Narayanamurti, E. Bucher and R. G. Maines, *Phys. Rev. Lett.*, 1970, **25**, 1430.
5 J. M. Lawrence, G. H. Kwei, J. L. Sarrao, Z. Fisk, D. Mandrus and J. D. Thompson, *Phys. Rev. B*, 1996, **54**, 6011.
6 J. R. Salvador, F. Guo, T. Hogan and M. G. Kanatzidis, *Nature*, 2003, **425**, 702; S. Margadonna, K. Prassides, A. N. Fitch, J. R. Salvador and M. G. Kanatzidis, *J. Am. Chem. Soc.*, 2004, **126**, 4498.
7 J. Arvanitidis, K. Papagelis, S. Margadonna, K. Prassides and A. N. Fitch, *Nature*, 2003, **425**, 599; J. Arvanitidis, K. Papagelis, S. Margadonna and K. Prassides, *Dalton Trans.*, 2004, 3144; S. Margadonna, J. Arvanitidis, K. Papagelis and K. Prassides, *Chem. Mater.*, 2005, **17**, 4474.
8 J. R. Salvador, D. Bilc, S. D. Mahanti, T. Hogan, F. Guo and M. G. Kanatzidis, *J. Am. Chem. Soc.*, 2004, **126**, 4474.

